A Complex Landslide in Ichinose Area Triggered by the 2024 Noto Peninsula Earthquake in Japan

Gonghui Wang[1*], Jiangkun He[2], Gen Furuya[3], Issei Doi[1], Koichi Hhayashi[1], and Yasuhiko OKADA[4]

[1]Disaster Prevention Research Institute, Kyoto University, Japan
[2]Graduate School of Science, Kyoto University, Japan
[3]Toyama Prefectural University, Japan
[4]Forestry and Forest Products Research Institute Japan, Japan

(*Corresponding E-mail: wang.gonghui.3r@kyoto-u.ac.jp)

Abstract: During the 2024 Noto Peninsula Earthquake (M_W7.5) in Japan, many landslides of different types and scales occurred, resulting in great damage to local properties and casualties. In this s Wang tudy, we introduce a large-scale landslide occurring in Ichinose area, Wajima City. This landslide originated from an old landslide, and the displaced landslide mass showed complex landsliding behavior. Through field geological and geophysical surveys and geotechnical examinations, the features of this landslide were detailed, and the possible initiation and movement mechanisms were examined. The main findings will be reported in this study.

Keywords: ***2024 Noto Peninsula Earthquake, Ichinose landslide, Complex landsliding phenomena, Liquefaction.***

Introduction

During the 2024 Noto Peninsula Earthquake in Japan, more than 6,000 landslides were triggered, including a large-scale event in the Ichinose area of Wajima City, Ishikawa Prefecture. This landslide exhibited high mobility, traveling more than 1 km, destroying several houses, and causing one fatality. To investigate its initiation and movement mechanisms, we conducted field surveys, microtremor measurements, and seismic monitoring, and collected soil samples from multiple locations within the landslide for laboratory testing. This study introduces some features of this landslide and reports some experimental examination results.

Ichinose landslide

The lithology at the head of the Ichinose landslide is dominated by conglomerate, tuffaceous sandstone, and andesitic pyroclastic rocks, whereas the middle to lower portions consists mainly of alternating sandstone, mudstone, and conglomerate. Field investigations suggest that the Ichinose landslide involved the movement of three distinct source areas, as schematically illustrated in Figure 1a. First, instability was triggered in Area 1 (Figure 1b), where the lower part of the slope fluidized, generating a debris flow approximately 6 m thick that traveled downslope and was deposited in residential areas about 600 m from the landslide toe. Second, the wedge-shaped Source Area 2 (Figure 1c) failed, and its mass was deposited at the base of the main scarp. Finally, Source Area 3 (Figure 1d) failed, with part of the displaced material deposited in a lateral gully and the remainder deposited on the exposed sliding surface of Source Area 1. Notably, the fluidization of the toe in Area 1 greatly amplified the destructive impact of the event. This sequence of failures underscores the complex, multi-stage nature of the Ichinose landslide.

Figure 1, (a) Overview of Ichinose landslide; (b) –(d) Close-up Views of different locations of source area.

Experimental examination

To investigate the initiation and movement mechanisms of the landslide, soil samples were collected from different locations and tested using a ring shear apparatus developed at Kyoto University. Undrained cyclic loading tests and drained monotonic shear tests were conducted to examine the undrained shear behavior and residual strengths of three samples (S1–S3), that were taken from the bottom of the landslide deposits at the outcropped sliding surface in Source Area 1, the upper part of the deposits near S1, and the distal toe part of the deposits, respectively. In the saturated undrained cyclic loading tests, each loading sequence consisted of 40 cycles at a frequency of 0.5 Hz, and if no failure occurred, an additional 40 cycles were applied. The test conditions are summarized in Table 1.

Table 1, Test condition.

	Normal stress (kPa)	Shear stress (kPa)	Cyclic loading (kPa)	Frequency (H_Z)	Density (g/cm^3)
S1	373	100	50, 75, 100, 115	0.5	1.18
S2	373	100	50, 60, 90, 115	0.5	0.98
S3	277	80	50, 75, 90	0.5	1.15

Results and Discussion

Representative test results are shown in Figures. 2–4. The test on S1 (clayey soil sampled from the sliding surface layer originated from Source Area 3) demonstrated that shear failure occurred only after prolonged cyclic loading, accompanied by a gradual increase in pore-water pressure (PWP), indicating a relatively low liquefaction potential. In contrast, S2 (sandy soil) exhibited shear failure within the same loading duration but with a rapid buildup of PWP, suggesting a higher liquefaction potential. The test on S3 (sandy soil) showed shear failure after a shorter loading duration, with a moderate increase in PWP, also indicating a relatively high liquefaction potential.

The test results for S1 indicate that the material from Source Area 3 has very low liquefaction potential. The residual shear strength of S1 also presents diverse shear rate-dependent behavior (Figure 5), showing that S1 is unlikely to fail solely under seismic loading. However, given the relatively steep slope of Source Area 3, failure of Source Area 2 could create a free face at its toe, potentially destabilizing the mass and inducing slides. This interpretation is consistent with field investigation findings. Comparison of the three test results further shows that S3 exhibits the lowest resistance to cyclic loading and is therefore most susceptible to liquefaction under seismic or other dynamic disturbances. This suggests that the toe area was the most likely to undergo liquefaction, which may explain the fluidized landsliding behavior observed in video recordings.

Conclusion

This study, based on field surveys, microtremor observations and ring shear test, yielding the following conclusions preliminarily:

(a) The Ichinose landslide exhibited multi-phase movement. Initially, the main body of the slope was destabilized by the earthquake, showing overall sliding behavior, while the toe part displayed fluidized movement associated with high water content. Subsequently, a wedge-shaped sliding mass at the slope crest failed and accumulated at the base of the scarp that was outcropped with movement of Source area 1. Finally, a shallow landslide at the ridge became unstable, with part of the displaced material deposited in a lateral gully and the remainder deposited on the exposed sliding surface of Source Areas 2 and 1.

(b) Under similar stress conditions as in-situ, materials near the slip zones in Areas 2 and 3 exhibited high resistance to liquefaction. Sandy soil derived from sandstone was susceptible to high pore-water pressure buildup; however, strong seismic energy would be required to induce the failure. In contrast, sandy soils from the toe deposits showed the lowest resistance to liquefaction, consistent with the observation that only the toe zone underwent fluidized behavior.

It should be noted that further analyses of the ground motion and the initiation processes of the landslides are ongoing, and the results will be reported in due course.

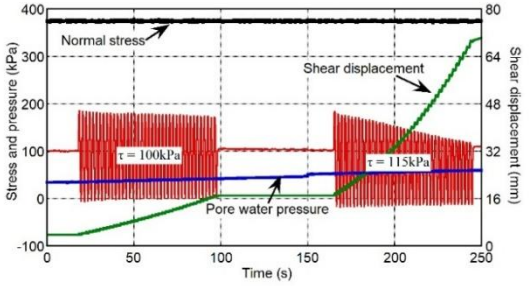

Figure 2, Undrained cyclic shear loading test on S1.

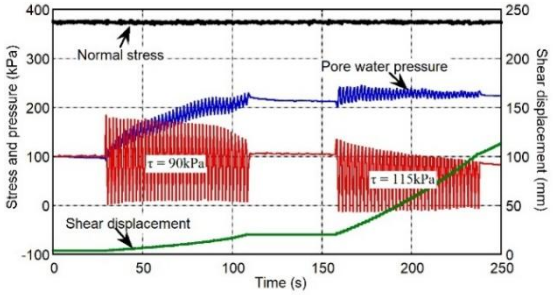

Figure 3, Undrained cyclic shear loading test on S2.

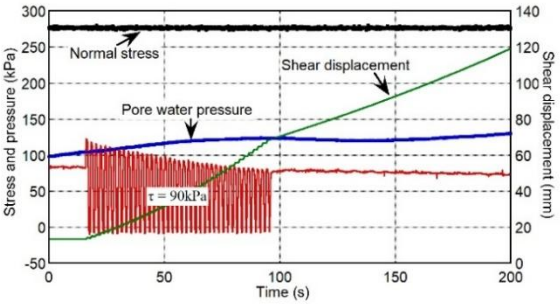

Figure 4, Undrained cyclic shear loading test on S3.

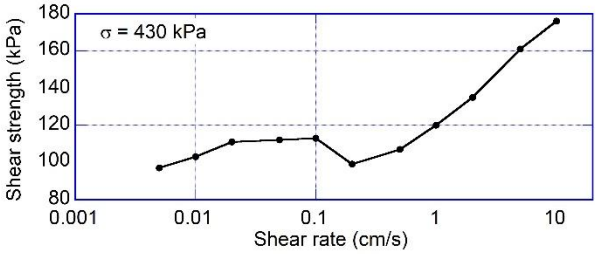

Figure 5, Residual shear strength of S1.

Acknowledgement

This work was supported by the collaborative research projects (2024IG-04 and 2025KG-03) of the Disaster Prevention Research Institute of Kyoto University.